Am J Transl Res 2020;12(2):551-562
www.ajtr.org /ISSN:1943-8141/AJTR0102962

Original Article

Y-320, a novel immune-modulator, sensitizes multidrug-resistant tumors to chemotherapy

Jiawei Hong[1,2*], Shilei Jing[1,2*], Yanpeng Zhang[1,2], Ronggao Chen[1,2], Kwabena Gyabaah Owusu-Ansah[1,2], Bingjie Chen[1,2], Haiyang Xie[1,2,3,4,5], Lin Zhou[1,2,3,4,5], Shusen Zheng[1,2,3,4,5], Donghai Jiang[1,2,3,4,5]

[1]Department of Surgery, Division of Hepatobiliary and Pancreatic Surgery, First Affiliated Hospital, School of Medicine, Zhejiang University, Hangzhou 310000, China; [2]NHFPC Key Laboratory of Combined Multi-Organ Transplantation, Hangzhou 310000, China; [3]Key Laboratory of The Diagnosis and Treatment of Organ Transplantation, CAMS, Beijing, China; [4]Key Laboratory of Organ Transplantation, Hangzhou 310003, Zhejiang Province, China; [5]Collaborative Innovation Center for Diagnosis Treatment of Infectious Diseases, Hangzhou 310000, China. [*]Equal contributors.

Received September 28, 2019; Accepted January 7, 2020; Epub February 15, 2020; Published February 28, 2020

Abstract: Y-320, a novel immune-modulator, inhibits IL-17 production by $CD4^+$ T cells stimulated with IL-15. Its use in autoimmune diseases such as rheumatoid arthritis has been documented. However, no studies have be conducted to evaluate its application in cancer treatment either as mono or combined therapy. This study demonstrated that while Y-320 had little effect on multidrug resistance (MDR) cell lines, it induced remarkable injury to MDR tumor cells when concurrently administered with other chemotherapeutic agents. Concomitant use of Y-320 with a low dose of paclitaxel significantly sensitized MDR tumors by inducing G2/M phase arrest and apoptosis. Further analyses indicated that Y-320 was a substrate of P-glycoprotein (P-gp). It could inhibit P-gp efflux function without altering P-gp expression, and subsequently reverse P-gp mediated drug resistance in MDR cells. The co-administration of Y-320 and paclitaxel suppressed tumor growth remarkably with an inhibition rate of 77.1% compared to 6.5% in the paclitaxel monotherapy group *in vivo*. This co-treatment did not increase extra complications in MDR tumor xenograft models. Particularly, no significant changes in body weight and hepatorenal serology were observed with the co-treatment. In conclusion, our results confirm that Y-320 is a promising chemotherapy sensitizer for the first time. The co-administration of Y-320 and chemotherapeutic agents might be an effective and low-toxicity chemotherapeutic regime for the MDR tumor patients.

Keywords: Y-320, multidrug resistance, P-glycoprotein, chemotherapy sensitizer, combined therapy

Introduction

Chemotherapy is one of the most widely used methods for treating malignant tumors. However, the extensive use of these agents in the clinic has resulted in a growing number of problems. Multidrug resistance (MDR) and the associated complications related to drug toxicity are of particular concern. Although high doses of chemotherapeutic agents play a remarkable role in killing tumors, they often induce many complications such as myelosuppression, weight loss, gastrointestinal dysfunction, nervous system dysfunction, cardiopulmonary dysfunction, hepatic and renal dysfunction. These undesirable effects have negatively impacted clinical treatment countermeasures for malignant and metastatic tumors. Alternatives such as low-dose multi-cycle therapeutic plan can mitigate these adverse reactions but can lead to drug resistance in tumors, further desensitizing these cells. As a result, balancing the effectiveness and low-toxicity of these agents is critical in the area of clinical research.

1-(4-chlorophenyl)-N-[3-cyano-4-(4-morpholinopiperidin-1-yl)phenyl]-5-methylpyrazole-4-carboxamide (Y-320), a novel phenylpyrazoleanilide immunomodulator [1, 2], can inhibit the synthesis of interleukin-17 (IL-17) in $CD4^+$ T cells [2]. IL-17 is an inflammatory cytokine with powerful pro-inflammatory properties, mediating various autoimmune diseases through diverse

mechanisms [3-7]. For example, IL-17 can stimulate interleukin 6 (IL-6) and CXCL1 expression which promotes inflammatory responses [3]. Studies have shown that collagen-induced arthritis (CIA) in mice and cynomolgus monkeys can be ameliorated with Y-320 by suppressing the biosynthesis of IL-17 [2]. Additionally, IL-17 has been shown to activate Src/PI3K/Akt/(NF-κB), MAPK, STAT3, and COX-2 pathways and participates in tumorigenesis, angiogenesis, and metastasis [8, 9]. For instance, the activation of the STAT3 pathway by IL-17 enhances the expression of anti-apoptotic genes such as Bcl-2, A1, and Mcl1 [10]. IL-17 can also promote the resistance of breast tumors to paclitaxel and docetaxel by activating the ERK1/2-STAT3-Bcl-2 axis signal pathway [11]. Therefore, the development of cisplatin resistance in colorectal cancer has also been linked to the expression IL-17. These findings suggest that inhibiting the function of IL-17 might have a beneficial effect on the treatment of malignant tumors. Consequently, the development of IL-17 inhibitors such as Y-320 holds promise in the tumor treatment strategy. To the best of our knowledge, no study has reported the oncological use of Y-320, either as mono or combination therapy. Moreover, the therapeutic efficacy and molecular mechanism of Y-320 in tumor treatment are not well understood yet.

In this study, we found that Y-320 exerted little effect on various cancer cells at concentrations less than 500 nM as monotherapy. Interestingly, the co-administering 500 nM Y-320 with cytotoxic agents (paclitaxel, vinorelbine, and doxorubicin) remarkably suppressed tumor growth in vitro. Co-treatment with a tolerable dose of Y-320 notably improved the effectiveness of paclitaxel in vivo with minimal systematic toxicity. For the first time, our findings demonstrate that Y-320 can be used as a promising drug in enhancing the anti-tumor effect of chemotherapeutic agents. Likewise, the co-administration of Y-320 and chemotherapeutic agents might be an effective and safe chemotherapeutic regime for patients with MDR tumors.

Materials and methods

Cell culture and mice

BCap37, Bads-200, and Bats-72 cells were maintained in RPMI 1640 medium supplemented with 10% fetal bovine serum (FBS), whereas Bads-200 was cultured with additional 200 nM paclitaxel. Huh7-TS-48 was maintained in minimum essential medium with 10% FBS. Female athymic nude (nu/nu) mice aged 4-5 weeks were purchased from the Animal Facility of Zhejiang University. All animal care and experiments were conducted according to the Guidelines of the Zhejiang University Animal Care Committee.

Drugs and treatments

Paclitaxel (injection, 5 mg/mL) was purchased from Mead Johnson Co. (Mead Johnson, USA). Vinorelbine (1 mg), doxorubicin (50 mg), 5-fluorouracil (100 mg), cisplatin (100 mg) were purchased from Dalian Meilun Biotechnology CO., LTD (Meilunbio, China). Y-320 (25 mg) was purchased from MedChemExpress Co. (MCE, China). Y-320 was dissolved in a mixture of alcohol and castor oil in a ratio of 1:1. Cells were evenly seeded in various plates or dishes in drug-free medium for 24 h. They were then treated with various doses of chemotherapeutic agents with or without co-administration of Y-320.

MTT assay and colony-forming assay

Cells were harvested and resuspended to a final concentration of 10^4 cells/ml. Aliquots of the cell suspension were evenly distributed into 96-well tissue culture plates. After overnight incubation, the designated columns were treated with various drug regimens. After 72 h incubation, MTT was added to detect cell viability. The medium containing MTT was replaced with 150 μL DMSO in each well to dissolve the formazan crystals after 4 h incubation. The absorbance in individual wells was determined at 570 nm using a microplate reader (Bio-Rad, USA).

Bads-200 cells were seeded into 6-cm dish at a density of 400 cells and were maintained with different drug regimens for 10 days. The cell clones were stained with Crystal Violet (CV). After washing the plates with PBS twice, the detached cells were fixed by methanol for 10 minutes and stained with CV for an additional 10 minutes.

Analysis of cell cycle

Cell cycle distribution was determined by flow cytometry. Briefly, after drug exposure for 72 h,

both detached and attached cells were harvested and washed twice with PBS, followed by fixation in 70% ethanol diluted in PBS. Cells were then incubated in PBS containing 100 μg/mL RNase-A and 40 μg/mL propidium iodide (PI) at room temperature for 0.5-1 h before flow cytometric analysis. Cell cycle distribution and DNA content were determined using a Coulter Epics V instrument (Beckman Coulter, USA).

Analysis of apoptosis

Annexin V/PI apoptosis detection kit (Beyotime, China) was used to detect cell apoptosis according to the manufacturer's instructions. Cells were harvested and washed twice with PBS after 48 h treatment. They were then suspended in 400 μL of binding buffer, 5 μL of Annexin V antibody conjugated with fluorescein isothiocyanate (FITC) and 10 μL of PI solution. After incubation in the mixture for 15 min at 4°C in the dark, the percentage of apoptotic cells was determined by flow cytometry.

Western blot analysis and antibodies

The Bads-200 cells were collected for western blot analysis after different treatments. The antibodies were listed as follows: GAPDH (db106), CDK1 (db2492), Cyclin B1 (db1172), CDK6 (db807), PKM2 (db2349), PARP (db1841), Cle-PARP (db3552), caspase-3 (db2059) from Diagbio Technology, LTD. (Diagbio, China); Cle-caspase-3 (ab2302) was obtained from Abcam plc. (Abcam, USA); goat anti-rabbit and goat anti-mouse IgG peroxidase-conjugated secondary antibodies (31460 and 31430) were purchased from Thermo-Pierce (Rockford, USA). Equal amounts (10 μg/lane) of proteins were separated on 10% SurePAGE gels (GenScript, China) and transferred to polyvinylidene difluoride membranes. The membranes were incubated with the respective antibodies mentioned above. After washing with 0.1% (v/v) Tween 20 in TBS, the membranes were incubated with peroxidase-conjugated goat anti-rabbit secondary antibodies followed by enhanced chemiluminescence staining.

Evaluation of therapeutic efficacy in vivo

Bats-72 cells ($1*10^6$ cells in 0.1 mL PBS) were implanted into the right flanks of the homozygous nude athymic mice (female, 4-5 weeks old). Three days after implantation, mice were randomly divided into 4 groups and treated with different regimens: (i) vehicle; (ii) Y-320 alone at 5 mg/kg, i.v.; (iii) paclitaxel alone at 15 mg/kg, i.v.; (iv) combination of Y-320 and paclitaxel. The same treatment regimens were repeated every 3 days for a total of 6 cycles. Two perpendicular diameters [width (W) and length (L)] of the tumors, as well as the body weight of mice, were measured every 3 days until the animals were sacrificed. The tumor volume (V) was roughly estimated according to the following formula: $V=(\pi*L*W^2)/6$.

After the animals were sacrificed, the tumor tissues were resected and weighed. At the same time, livers, kidneys and blood samples were harvested. Serum alanine aminotransferase (ALT) and creatinine (Cr) levels were measured using a Hitachi 7600 automatic analyzer (Hitachi, Japan). The inhibition rate (IR) of tumor growth was calculated according to the following formula: IR=100%* (mean tumor weight of the control group-mean tumor weight of the experimental group)/mean tumor weight of the control group.

Rhodamine 123 efflux assay

Bads-200 cells were incubated with vehicle medium, Y-320 or verapamil for 3 h. Afterwards, 5 μM Rhodamine 123 (Meilunbio, China) was added in each group. The cells were then incubated for an additional 0.5 h. After washing with cold PBS, the cells were trypsinized and resuspended in 400 μL PBS. Intracellular Rhodamine 123 (Rh123) fluorescence intensity was determined with Coulter Epics V instrument (Beckman Coulter, USA).

P-glycoprotein ATPase activity assay

The P-gp-Glo™ Assay Systems (Promega, USA) provided the necessary reagents for performing luminescent P-glycoprotein (P-gp) ATPase assays. The P-gp-Glo™ Assay relied on the ATP-dependence of the light-generating reaction of firefly luciferase, which was a valuable screening tool for determining if a drug interacted with P-gp. This assay system consisted of human P-gp/MDR1 membrane and P-gp/MDR1 negative control membrane fractions, buffers, solutions, and relevant reagents. The effects of Y-320 on the ATPase activity of P-glycoprotein were measured according to the protocol provided by the manufacturer.

Statistical analysis

Results were presented as means ± standard errors. The difference was considered statistically significant at a level of $P<0.05$ or $P<0.01$, and statistical power was set at 0.80. Student's t-test was used for two-group comparisons, and multiple-treatment groups were analyzed by one-way analysis of variance (ANOVA). Statistical analysis of the data presented was performed using SPSS version 22.0 (SPSS, USA).

Results

Y-320 reverses the resistance to paclitaxel in MDR cancer cells

The structural formula of Y-320 is shown in **Figure 1A**. We first determined the half-maximal inhibitory concentration of Y-320 in Bats-72, Bads-200 and Huh7-TS-48. As shown in **Figure 1B**, Y-320 had little cytotoxicity from 0 to 500 nM, and the survival rate for each cell line was more than 80%. Hence, 500 nM Y-320 was chosen to combine with various chemotherapeutic agents to evaluate the anticancer effects. The MDR cell lines Bats-72, Bads-200 and Huh7-TS-48 are known to be highly resistant to paclitaxel [12, 13]. As shown in **Figure 1C-H**, Y-320 could significantly improve the cytotoxicity of paclitaxel in three MDR cell lines. Compared to paclitaxel alone, the reversal index (RI) of Y-320 combined with paclitaxel was 5.5 (Bads-200), 9.4 (Bats-72) and 1.7 (Huh7-TS-48), respectively. These results confirmed that adding Y-320 to the regimen significantly sensitized MDR cancer cells to paclitaxel. Furthermore, colony-forming assay was conducted to further determine whether the co-treatment could improve the cytotoxicity of paclitaxel. As shown in **Figure 1I**, the colony-forming assay clearly showed that the number and size of colonies were drastically reduced in the co-treatment group compare with CTL and monotherapy groups. These results demonstrated that Y-320 had remarkably reversal effects when combined with paclitaxel or other chemotherapeutic agents in MDR cancer cells.

Y-320 enhances paclitaxel-induced G2/M arrest

As depicted in **Figure 2A**, the morphology of Bads-200 did not significantly change after 72 h treatment with paclitaxel or Y-320 alone. However, co-treatment with Y-320 and paclitaxel resulted in obviously abnormal morphology, evidenced by suspending cells, cytoplasmic blebs, and apoptotic bodies. As paclitaxel had been shown to cause mitotic arrest and lead to apoptosis in various tumor cells [14], we explored the effect of this co-treatment on the cell cycle as well. Compared with monotherapies of 500 nM Y-320 or paclitaxel alone, concurrent treatment of Y-320 and paclitaxel significantly increased the percentage of cells at G2/M phase, from 6.3% to 42.5% (**Figure 2B**, **2C**). Furthermore, we also analyzed the levels of CDK1, CDK6, PKM2, and Cyclin B1, all of which had been shown to have a close correlation with G2/M arrest [15-19]. As shown in **Figure 2D**, the levels of CDK1, CDK6 and PKM2 were significantly down-regulated while Cyclin B1 levels increased in the co-treatment group (The Original image of WB scan is shown in the Supplementary Figures 1, 2, 3, 4 and 5). In conclusion, our results clearly showed that co-administration with Y-320 could enhance paclitaxel-induced G2/M arrest.

Y-320 enhances paclitaxel-induced tumor cell apoptosis

Paclitaxel has been closely related to the apoptosis of various tumor cells [20, 21], which was confirmed by Annexin V/propidium iodide apoptosis detection assay. As depicted in **Figure 3A**, **3B**, the results indicated that co-treatment of Y-320 and paclitaxel significantly increased the ratio of apoptotic Bads-200 cells compared to paclitaxel monotherapy group (30.8% versus 2.2%, $P<0.01$). Subsequently, the expression level of several regulatory proteins associated with apoptosis was analyzed by western blot. As shown in **Figure 3C**, the levels of poly ADP-ribose polymerase (PARP) and cleavage of caspase-3 were significantly increased in the co-treatment group (The Original image of WB scan is shown in the Supplementary Figures 6, 7, 8, 9 and 10). In conclusion, this co-administration enhanced paclitaxel-induced tumor cell apoptosis.

Y-320 is a substrate of P-gp reverses MDR by inhibiting P-gp function

In our previous study, we proved that both Bads-200 and Bats-72 cell were not only resistant to paclitaxel but also resistant to docetax-

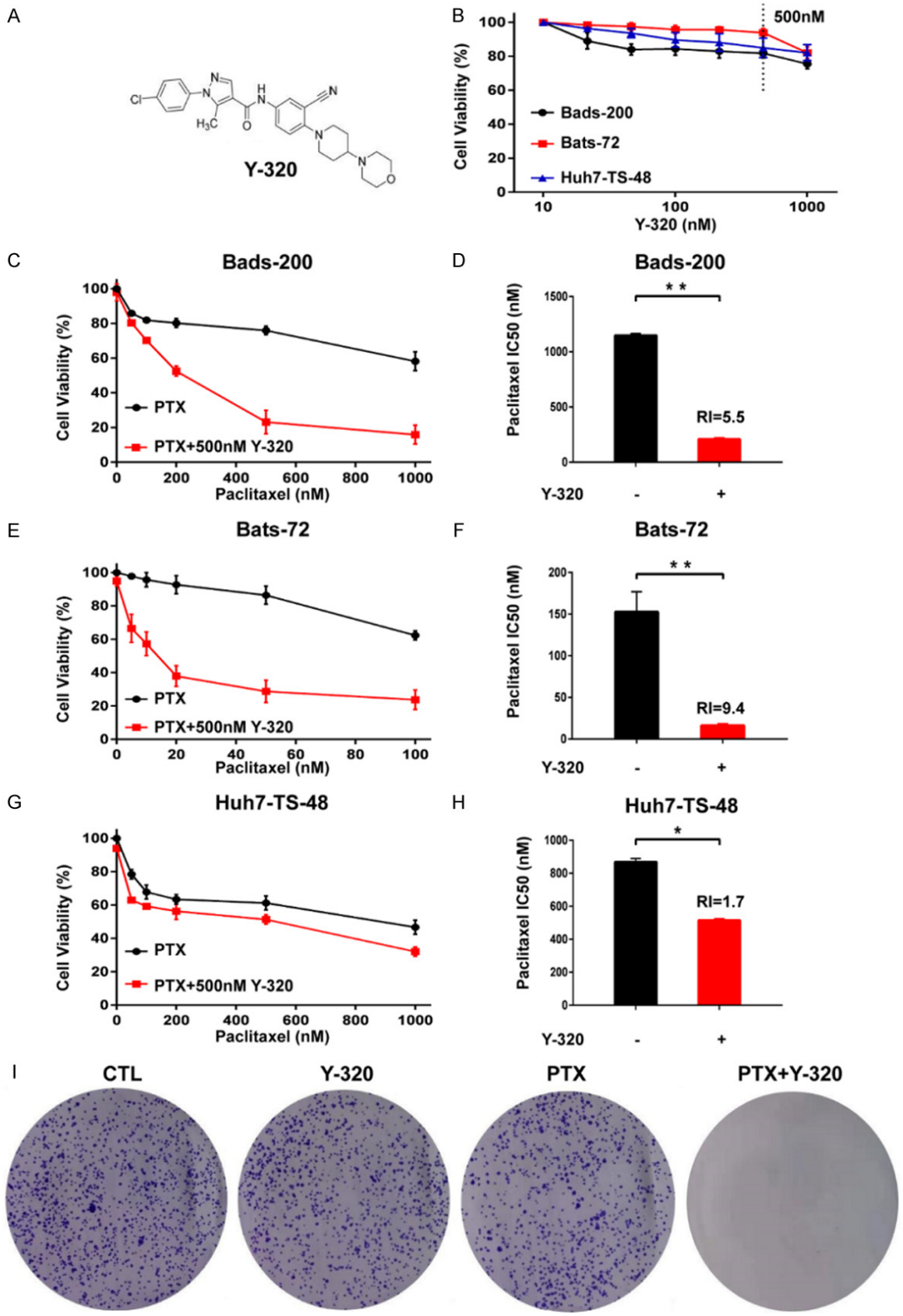

Figure 1. Y-320 reverses the resistance to paclitaxel in various MDR cancer cells. A. The structural formula of Y-320. B. Bads-200, Bats-72 and Huh7-TS-48 were incubated with increasing doses of Y-320 alone for 72 h. C-H.

Bads-200, Bats-72 and Huh7-TS-48 were exposed to a series of concentrations of paclitaxel with or without 500 nM Y-320 for 72 h. The IC_{50} of paclitaxel was determined with or without 500 nM Y-320 after 72 h treatment. The reversal index of Y-320 combined with paclitaxel was also calculated compared with paclitaxel group. I. Colony formation of Bads-200 with various treatments. Data are shown as mean ± SD. Student's t-test was used for two-group comparisons. *P<0.05; **P<0.01; CTL, control; Y-320, 500 nM Y-320; PTX, 500 nM paclitaxel; PTX+Y-320, combination of 500 nM paclitaxel and 500 nM Y-320; RI, reversal index.

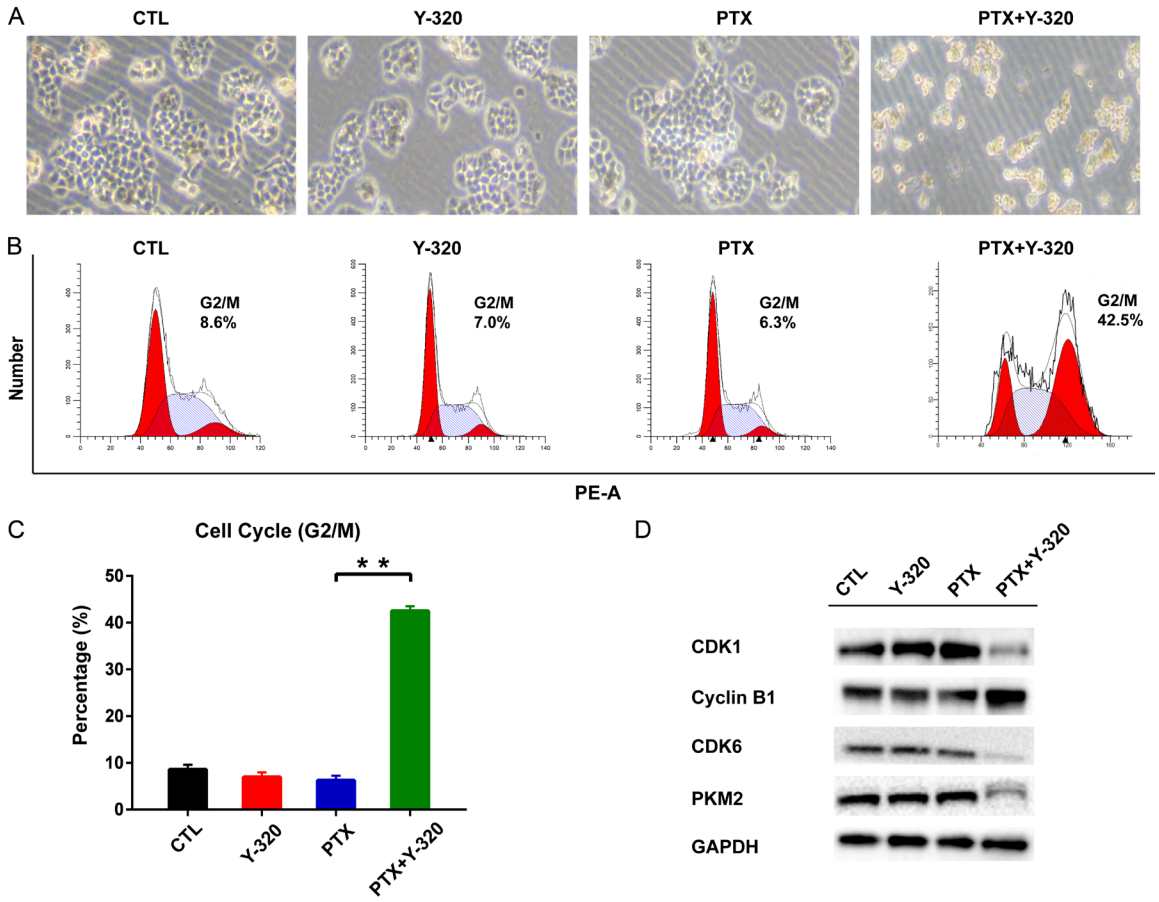

Figure 2. Y-320 enhances paclitaxel-induced G2/M block of tumor cell cycle. A. Morphological images of Bads-200 taken with an inverted microscope (×100) after different treatments for 72 h. B, C. Cell cycle analysis of Bads-200 after different treatments for 72 h and the G2/M phase histogram. D. Western blot analysis of cell cycle-related proteins, CDK1, Cyclin B1, CDK6 and PKM2 in Bads-200. Data are shown as mean ± SD. Student's t-test was used for two-group comparisons. *P<0.05; **P<0.01; CTL, control; Y-320, 500 nM Y-320; PTX, 500 nM paclitaxel; PTX+Y-320, combination of 500 nM paclitaxel and 500 nM Y-320.

el, vinorelbine, and doxorubicin. Further investigation of the reversal activity of Y-320 with these chemotherapeutic agents was conducted. As shown in **Table 1**, the co-administration of Y-320 remarkably enhanced the cytotoxic profile when combined with vinorelbine and doxorubicin in Bads-200 cells. The reversal indexs (RI) were 20.6 and 34.8, respectively. Conversely, the co-treatment of Y-320 showed little reversal effect when combined with 5-fluorouracil and cisplatin. The results obtained in Bats-72 were similar to Bads-200. Altering P-gp expression or its function can reverse the P-gp mediated MDR, improving the efficacy of chemotherapy. Therefore, we further explored whether the synergistic effect of Y-320 and paclitaxel was caused by the down-regulation of P-gp protein or the inhibition of its function. As shown in **Figure 4A**, Bads-200, Bats-72 and Huh7-TS-48 had a high P-gp expression. Y-320 did not influence the expression of P-gp protein (**Figure 4B**) (The Original image of WB scan in **Figure 4A**, **4B** is shown in the Supplementary Figures 11, 12, 13 and 14). Moreover, we per-

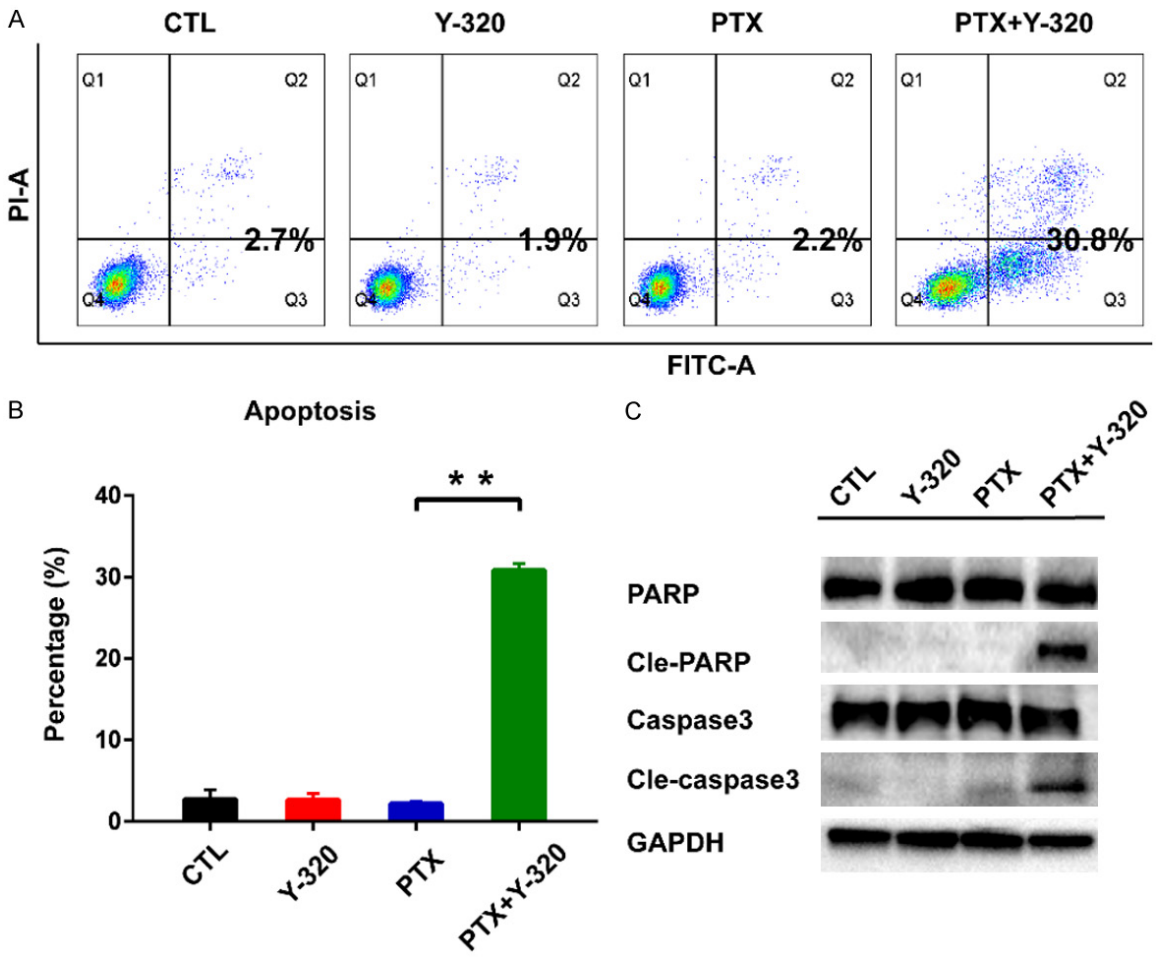

Figure 3. Y-320 enhances paclitaxel-induced tumor cell apoptosis. A, B. Apoptosis assay of Bads-200 after different treatments for 72 h. C. Western blot analysis of apoptosis-related proteins, PARP, C-PARP, Caspase3 and C-Caspase3 in Bads-200. Data are shown as mean ± SD. Student's t-test was used for two-group comparisons. *P<0.05; **P<0.01; CTL, control; Y-320, 500 nM Y-320; PTX, 500 nM paclitaxel; PTX+Y-320, combination of 500 nM paclitaxel and 500 nM Y-320.

Table 1. Y-320 sensitizes MDR breast cancer cells to chemotherapy agents

Drug	Y320 (nM)	Bads-200		Bats-72	
		IC_{50} (nM)	RI	IC_{50} (nM)	RI
Paclitaxel	+0	1148.1±13.1	-	152.8±19.6	-
	+500	208.3±91.0	5.5	16.2±1.7	9.4
Vinorelbine	+0	6736.1±69.4	-	26250.0±694.4	-
	+500	326.4±90.3	20.6	1111.1±416.7	23.6
Doxorubicin	+0	192129.6±463.0	-	1099.5±476.4	-
	+500	5523.3±290.7	34.8	324.1±163.7	3.4
5-Fluorouracil	+0	9306.7±139.6	-	43400.0±5200.0	-
	+500	9028.4±694.0	1.0	42800.0±300.0	1.0
Cisplatin	+0	1909.7±6.9	-	6220.2±29.8	-
	+500	1777.8±444.4	1.1	6090.3±6.9	1.0

Note: RI (reversal index) was determined by the IC_{50} in the absence of Y-320 divided by the IC_{50} in the presence of Y-320.

formed Rh123 intracellular accumulation and efflux assay to evaluate the effects of Y-320 on P-gp function. As shown in **Figure 4C**, **4D**, compared to the group without any inhibitor (ROD),

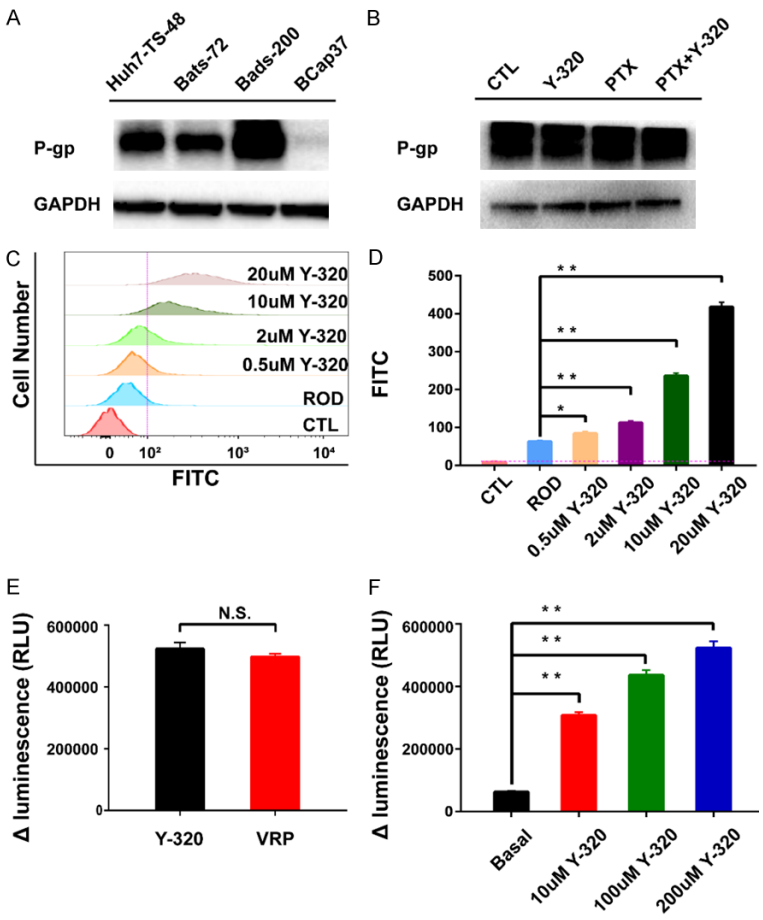

Figure 4. Y-320's mechanism for sensitizing cancer cells to chemotherapeutic agents. A. Western blot analysis of P-gp proteins in Bads-200, Bats-72, BCap-37 and Huh7-TS-48. B. Western blot analysis of P-gp proteins in Bads-200 after differential treatment for 72 h. C, D. Intracellular Rh123 fluorescence intensity in Bads-200 with different treatments. E. The effect of Y-320 on the ATPase activity of P-gp compared with verapamil. F. The effect of Y-320 on the ATPase activity of P-gp was measured in different concentrations. Data are shown as mean ± SD. Student's t-test was used for two-group comparisons. CTL, control; PTX+Y-320, combination of paclitaxel and Y-320. Rod, treatment with 5 μM rhodamine 123 for 0.5 h.

the amount of intracellular Rh123 in co-administration of Y-320 group was significantly increased in a dose-dependent manner. Subsequently, we used P-gp-Glo™ Assay to evaluate whether Y-320 was a substrate of P-gp. Compared to verapamil, a well-known substrate of P-gp, Y-320 had a similar effect on the ATPase activity of P-gp (**Figure 4E**). As shown in **Figure 4F**, Y-320 also stimulated P-gp ATPase activity in a dose-dependent manner, indicating that Y-320 could directly interact with P-gp. These findings suggested that Y-320 was a substrate of P-gp, and it could sensitize cancer cells to chemotherapy via inhibiting P-gp function without altering its expression level.

Y-320 sensitizes MDR xenograft tumor to paclitaxel in vivo

The previous results indicated that co-administration with Y-320 had reliable reversal effect *in vitro*. Hence, there was a clinical concern regarding whether this phenomenon could be replicated *in vivo*. As shown in **Figure 5A-C**, after six treatment cycles, control and monotherapy groups did not show significant difference in tumor volume or weight, whereas the co-administration group showed significantly reduced tumor volume and weight compared to the other three groups. The mean tumor volumes were 591.6±30, 617.4±38, 646.6±27 and 134.6±32 mm^3, and mean tumor weights were 0.926 ±0.22, 1.01±0.20, 0.866± 0.20, 0.212±0.14 g, respectively. Compared to the paclitaxel monotherapy group, the co-administration with Y-320 and paclitaxel suppressed tumor growth remarkably with an IR increased from 6.5% to 77.1%. Furthermore, resected Bats-72 xenograft tumors were analyzed by immunohistochemistry staining with Ki-67 antibody. When Y-320 was co-administered with paclitaxel, the number of Ki-67-positive cells was significantly reduced (**Figure 5D**). Particularly, the co-treatment did not exert any significant effects on body weight (**Figure 5E**). As shown in **Figure 5F**, **5G**, the mean serum ALT levels were 49.6±10.2, 49.0±9.8, 50.6±5.9 and 45.5±10.6 U/L, while the mean serum Cr levels were 4.9±0.9, 4.3±0.4, 4.9±0.6 and 4.5±0.6 U/L, respectively. Therefore, the results of serological studies showed that there was little adverse effects on the liver and kidney function after the combination therapy. In conclusion, our results proved that the co-administration of Y-320 and paclitaxel markedly inhibited tumor growth in Bats-72 xenografts without severe adverse effects.

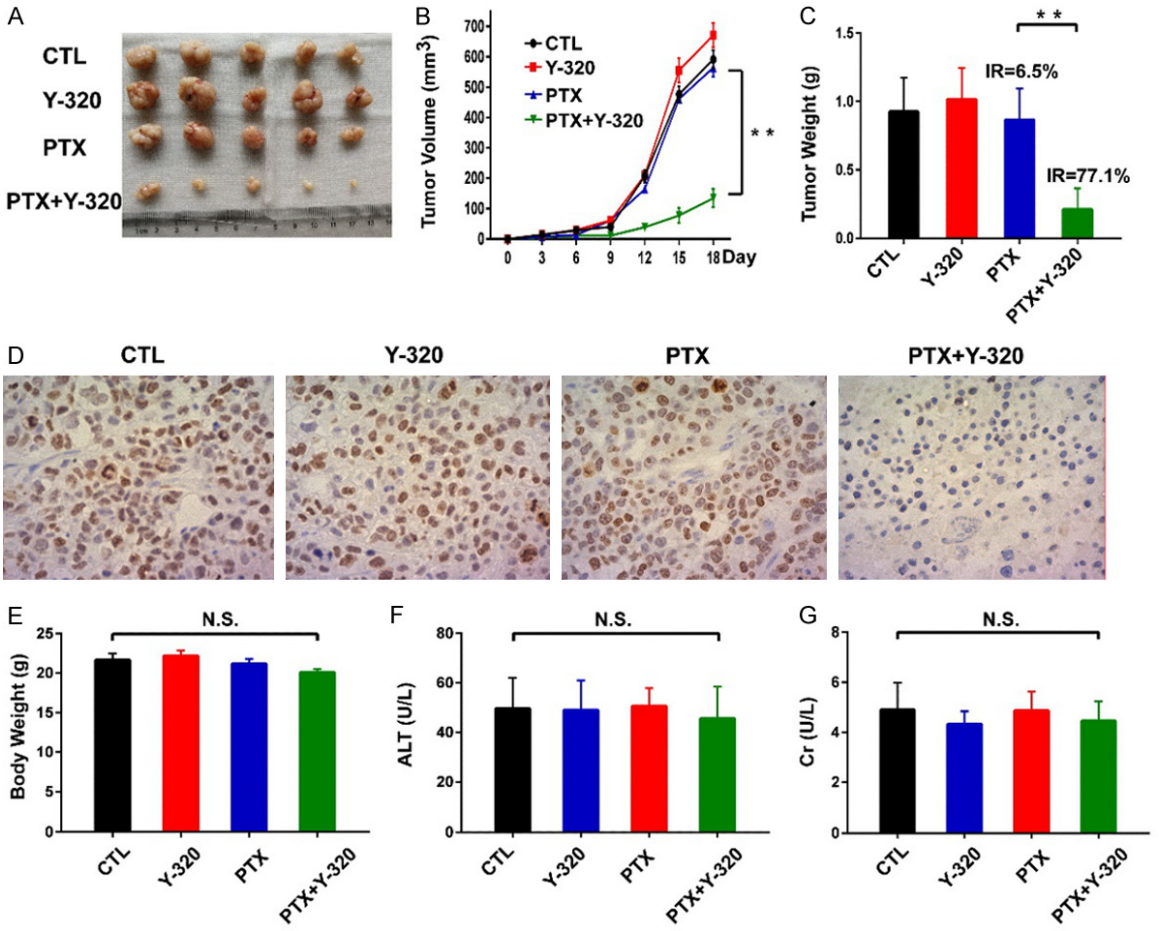

Figure 5. The co-administration with Y-320 improves the effectiveness of paclitaxel in Bats-72 xenograft models without additional adverse effects. Nude mice bearing Bats-72 tumors were treated with paclitaxel +/-Y-320. A. Tumor mass compared among four groups with different treatments. B. Tumor volume of the four groups in the process. C. Tumor weight compared among groups at the end of experiments. The inhibition rates of tumor gross in paclitaxel and co-treatment group were calculated compared with the control group. D. Ki-67 immunohistochemical staining (×200) of tumor. E. Body weight of mice at the end of experiment. F, G. Serum ALT and Cr levels measured in each group at the end of experiment. Data are shown as mean ± SD. Student's t-test was used for two-group comparisons, and multiple-treatment groups were analyzed by one-way ANOVA. N.S., P>0.05; *P<0.05; **P<0.01; CTL, control; PTX+Y-320, combination of paclitaxel and Y-320. IR, inhibition rate.

Discussion

Phenylpyrazolinamine compounds inhibit IL-17 production in murine and human $CD4^+$ T cells stimulated with IL-15 in a dose-dependent manner [1, 2]. One of such compounds, Y-320 exhibits the strongest inhibitory effect on IL-17 biosynthesis [1]. It has been reported that Y-320 can reduce mRNA expression of IL-17 in antigen-specific $CD4^+$ T cells in arthritic joints, leading to the delay of the joint destruction. Similarly, the plasma titer of anti-type II collagen IgG1 can be reduced by Y-320 in CIA mice. In mice and cynomolgus monkey models, Y-320 ameliorates collagen-induced arthritis [1, 2]. So far, these are the only published studies regarding the potential application of Y-320. In the present study, we discovered that Y-320 could improve the sensitivity of MDR tumor cells to lower doses of cytotoxic agents such as paclitaxel, vinorelbine, and doxorubicin. Furthermore, the co-administration of Y-320 and chemotherapeutics was able to enhance the therapeutic efficacy and generate synergistic anti-cancer effects *in vivo*. Better tolerance and lower chemotherapy-related adverse effects were observed in the co-treatment group compared to Y-320 monotherapy group. These results demonstrated that this co-administration could be an effective and low-toxic treatment strategy in

MDR cancers. To our knowledge, this study is the first to confirm that Y-320 is a valuable chemo-sensitizer in anti-cancer therapy.

The mechanisms involved in MDR include barriers to transport/uptake, dysfunction of drug activation, changes of agent target sites, new metabolic pathways of drugs, an increase of drug enzyme as well as the increase of drug efflux. P-gp is one of the major ATP-dependent efflux pumps responsible for tumor resistance to chemotherapeutic agents. It has been generally recognized that the inhibition of its expression or its function can reverse the P-gp mediated MDR and improve the efficacy of chemotherapy. Our data showed that Y-320 could inhibit P-gp function in a dose-dependent manner rather than influencing the expression of P-gp. Subsequently, P-gp-Glo™ assay demonstrated that Y-320 stimulates P-gp ATPase activity in purified recombinant human P-gp membrane protein. These findings confirmed that Y-320 is a substrate of P-gp. Thus, Y-320 could compete with chemotherapeutic agents for P-gp binding sites to increase the intracellular concentration of chemotherapeutic agents, thus improving the effectiveness of chemotherapy. In tumor xenograft assays, Y-320 sensitized MDR breast tumor to paclitaxel *in vivo*. Both Y-320 and paclitaxel monotherapies exerted little effects on tumor growth. When xenografts were treated with the combination of paclitaxel and Y-320, the inhibition rate of paclitaxel on Bats-72 tumors increased from 6.5% to 77.1%. Moreover, it has been documented that IL-17 plays a role in promoting the resistance of breast cancer cells against paclitaxel *in vivo*, suggesting that the inhibition of IL-17 might reverse the resistance to paclitaxel. However, whether the suppression of IL-17 by Y-320 directly contributes to sensitizing the MDR breast tumor to paclitaxel *in vivo* is still unclear. We aim to further investigate and verify this hypothesis in future.

Major success in the combination of therapeutic countermeasures against P-gp inhibitors and chemotherapeutic agents has been achieved over the past decade. Although traditional P-gp inhibitors (Verapamil, Ciclosporin A, etc.) can effectively inhibit the function of P-gp, they also generate adverse effects by interfering with normal physiological functions, leading to arrhythmia [22], gastrointestinal and nervous system dysfunctions. These effects limit the clinical application of P-gp inhibitors. On the contrary, Y-320 exhibits a favorable safety profile. Its co-administration with chemotherapeutic agents has demonstrated reduced toxicity without weight loss in nude mice models, as well as decreased hepatorenal injury. We speculate that the inflammatory regulation of Y-320 probably plays an important role in reducing the toxic side effects *in vivo* since the co-administration of immune-modulator and chemotherapy agents has been reported to reduce severe systemic toxicity. The immunological competence of immune modulators might contribute to the reduction of complications caused by cytotoxicity agents. Several studies have reported that the combined use of immune modulators and chemotherapeutic agents could improve the effectiveness of the latter [23-25], reduce the adverse effects [26, 27] and improve safety. Zhang Y's research showed that the immunomodulator JLNT could reduce diarrhea, hepatocellular injury and hepatic steatosis caused by oxaliplatin [27]. Immunomodulator, lipopeptide JBT-3002 has also been shown to prevent damage to the intestinal epithelium and lamina propria, thus reducing the frequency of diarrhea and other gastrointestinal complications caused by irinotecan in colorectal carcinoma patients [26, 28]. And immunomodulator lenalidomide monotherapy can lead to less hematologic toxicity compared with adjuvant chemotherapy for certain non-Hodgkin lymphoma (NHL) [23]. In light of this, further investigations need to be conducted to determine whether Y-320 could reduce the toxic side effect of paclitaxel by regulating IL-17 *in vivo*.

In a nutshell, our results showed that Y-320 could reverse P-gp-mediated MDR by inhibiting P-gp activity. Co-administration of Y-320 and chemotherapy drugs could significantly suppress MDR tumors without increasing toxicity *in vivo*. This combination might be appropriate for patients who are unresponsive to maximal dose of chemotherapeutic agents or in those unable to tolerate the associated systematic toxicity. This study may offer new insights into the clinical application of this novel immune-modulator in anticancer treatment infuture.

Acknowledgements

We thank Mrs. Rong Su for providing the flow cytometry technology. We thank Mr. Cheng Jin

and Mrs. Mengqiao Zhou for providing the xenograft technology of athymic nude mice. We thank the support of Zhejiang Provincial Natural Science Foundation (LY18H160017), Fundamental Research Funds for the Central Universities (2019XZZX005-1-08), Innovative Research Groups of National Natural Science Foundation of China (No. 81721091), National S&T Major Project (No. 2017ZX10203205), Zhejiang International Science and Technology Cooperation Project (NO. 2016C04003).

Disclosure of conflict of interest

None.

Address correspondence to: Shusen Zheng and Donghai Jiang, Department of Surgery, Division of Hepatobiliary and Pancreatic Surgery, First Affiliated Hospital, School of Medicine, Zhejiang University, No. 79, Qingchun Road, Shangcheng District, Hangzhou, Zhejiang Province, China. Tel: +86-571-87236567; Fax: +86-571-87236466; E-mail: shusenzheng@zju.edu.cn (SSZ); jdh8499@zju.edu.cn (DHJ)

References

[1] Ushio H, Ishibuchi S, Adachi K, Oshita K and Chiba K. Phenylpyazoleanilides as potent inhibitor of IL-15 dependent T cell proliferation. Part 2: discovery of a new drug candidate, Y-320. Lett Drug Des Discov 2008; 5: 292-296.

[2] Ushio H, Ishibuchi S, Oshita K, Seki N, Kataoka H, Sugahara K, Adachi K and Chiba K. A new phenylpyrazoleanilide, y-320, inhibits interleukin 17 production and ameliorates collagen-induced arthritis in mice and cynomolgus monkeys. Pharmaceuticals (Basel) 2013; 7: 1-17.

[3] Chang SH and Dong C. A novel heterodimeric cytokine consisting of IL-17 and IL-17F regulates inflammatory responses. Cell Res 2007; 17: 435-440.

[4] Kim BS, Park YJ and Chung Y. Targeting IL-17 in autoimmunity and inflammation. Arch Pharm Res 2016; 39: 1537-1547.

[5] Kolls JK and Linden A. Interleukin-17 family members and inflammation. Immunity 2004; 21: 467-476.

[6] Park H, Li Z, Yang XO, Chang SH, Nurieva R, Wang YH, Wang Y, Hood L, Zhu Z, Tian Q and Dong C. A distinct lineage of CD4 T cells regulates tissue inflammation by producing interleukin 17. Nat Immunol 2005; 6: 1133-1141.

[7] Weaver CT, Hatton RD, Mangan PR and Harrington LE. IL-17 family cytokines and the expanding diversity of effector T cell lineages. Annu Rev Immunol 2007; 25: 821-852.

[8] Ple C, Fan Y, Ait Yahia S, Vorng H, Everaere L, Chenivesse C, Balsamelli J, Azzaoui I, de Nadai P, Wallaert B, Lazennec G and Tsicopoulos A. Polycyclic aromatic hydrocarbons reciprocally regulate IL-22 and IL-17 cytokines in peripheral blood mononuclear cells from both healthy and asthmatic subjects. PLoS One 2015; 10: e0122372.

[9] Ryu H and Chung Y. Regulation of IL-17 in atherosclerosis and related autoimmunity. Cytokine 2015; 74: 219-227.

[10] Laprevotte E, Cochaud S, du Manoir S, Lapierre M, Dejou C, Philippe M, Giustiniani J, Frewer KA, Sanders AJ, Jiang WG, Michaud HA, Colombo PE, Bensussan A, Alberici G, Bastid J, Eliaou JF and Bonnefoy N. The IL-17B-IL-17 receptor B pathway promotes resistance to paclitaxel in breast tumors through activation of the ERK1/2 pathway. Oncotarget 2017; 8: 113360-113372.

[11] Punt S, Fleuren GJ, Kritikou E, Lubberts E, Trimbos JB, Jordanova ES and Gorter A. Angels and demons: Th17 cells represent a beneficial response, while neutrophil IL-17 is associated with poor prognosis in squamous cervical cancer. Oncoimmunology 2015; 4: e984539.

[12] Chen R, Cheng Q, Owusu-Ansah KG, Chen J, Song G, Xie H, Zhou L, Xu X, Jiang D and Zheng S. Cabazitaxel, a novel chemotherapeutic alternative for drug-resistant hepatocellular carcinoma. Am J Cancer Res 2018; 8: 1297-1306.

[13] Jiang D, Sui M, Zhong W, Huang Y and Fan W. Different administration strategies with paclitaxel induce distinct phenotypes of multidrug resistance in breast cancer cells. Cancer Lett 2013; 335: 404-411.

[14] Weaver BA. How Taxol/paclitaxel kills cancer cells. Mol Biol Cell 2014; 25: 2677-2681.

[15] Schmidt M, Rohe A, Platzer C, Najjar A, Erdmann F and Sippl W. Regulation of G2/M transition by inhibition of WEE1 and PKMYT1 kinases. Molecules 2017; 22.

[16] Chohan TA, Qayyum A, Rehman K, Tariq M and Akash MSH. An insight into the emerging role of cyclin-dependent kinase inhibitors as potential therapeutic agents for the treatment of advanced cancers. Biomed Pharmacother 2018; 107: 1326-1341.

[17] Gavet O and Pines J. Activation of cyclin B1-Cdk1 synchronizes events in the nucleus and the cytoplasm at mitosis. J Cell Biol 2010; 189: 247-259.

[18] Zhang Z, Deng X, Liu Y, Liu Y, Sun L and Chen F. PKM2, function and expression and regulation. Cell Biosci 2019; 9: 52.

[19] Li Q, Zhang D, Chen X, He L, Li T, Xu X and Li M. Nuclear PKM2 contributes to gefitinib resis-

tance via upregulation of STAT3 activation in colorectal cancer. Sci Rep 2015; 5: 16082.
[20] Xie S, Ogden A, Aneja R and Zhou J. Microtubule-binding proteins as promising biomarkers of paclitaxel sensitivity in cancer chemotherapy. Med Res Rev 2016; 36: 300-312.
[21] Ferlini C, Cicchillitti L, Raspaglio G, Bartollino S, Cimitan S, Bertucci C, Mozzetti S, Gallo D, Persico M, Fattorusso C, Campiani G and Scambia G. Paclitaxel directly binds to Bcl-2 and functionally mimics activity of Nur77. Cancer Res 2009; 69: 6906-6914.
[22] Saaby L, Tfelt-Hansen P and Brodin B. The putative P-gp inhibitor telmisartan does not affect the transcellular permeability and cellular uptake of the calcium channel antagonist verapamil in the P-glycoprotein expressing cell line MDCK II MDR1. Pharmacol Res Perspect 2015; 3: e00151.
[23] Galanina N, Petrich A and Nabhan C. The evolving role of lenalidomide in non-Hodgkin lymphoma. Leuk Lymphoma 2016; 57: 1507-1516.
[24] Konovalova NP. Ultralow doses of various drugs in chemotherapy of experimental tumors. Bull Exp Biol Med 2003; 135 Suppl 7: 45-47.
[25] Mickey DD. Combined therapeutic effects of an immunomodulator, PSK, and chemotherapy with carboquone on rat bladder carcinoma. Cancer Chemother Pharmacol 1985; 15: 54-58.
[26] Shinohara H, Bucana CD, Killion JJ and Fidler IJ. Intensified regression of colon cancer liver metastases in mice treated with irinotecan and the immunomodulator JBT 3002. J Immunother 2000; 23: 321-331.
[27] Zhang Y, Li Q, Wang J, Cheng F, Huang X, Cheng Y and Wang K. Polysaccharide from Lentinus edodes combined with oxaliplatin possesses the synergy and attenuation effect in hepatocellular carcinoma. Cancer Lett 2016; 377: 117-125.
[28] Shinohara H, Killion JJ, Kuniyasu H, Kumar R and Fidler IJ. Prevention of intestinal toxic effects and intensification of irinotecan's therapeutic efficacy against murine colon cancer liver metastases by oral administration of the lipopeptide JBT 3002. Clin Cancer Res 1998; 4: 2053-2063.

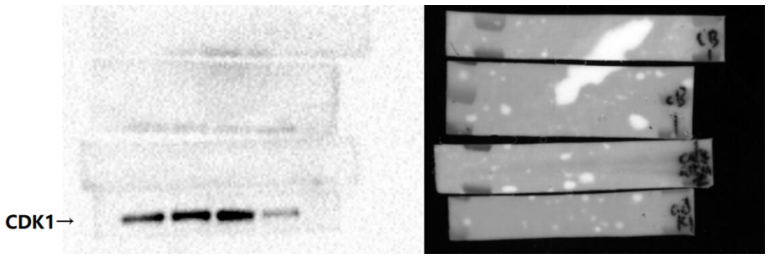

Supplementary Figure 1. The original full scan the entire original gel for CDK1 in **Figure 2D**.

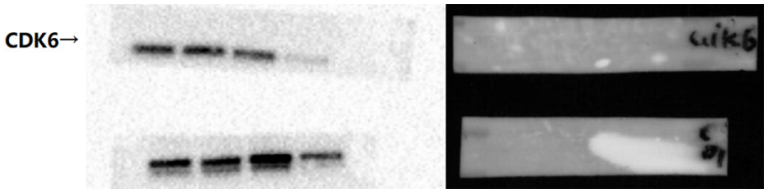

Supplementary Figure 2. The original full scan the entire original gel for CDK6 in **Figure 2D**.

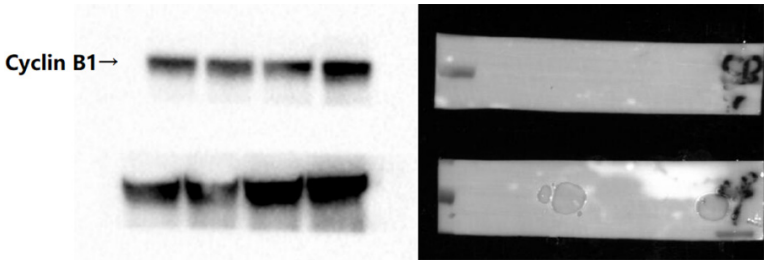

Supplementary Figure 3. The original full scan the entire original gel for Cyclin B1 in **Figure 2D**.

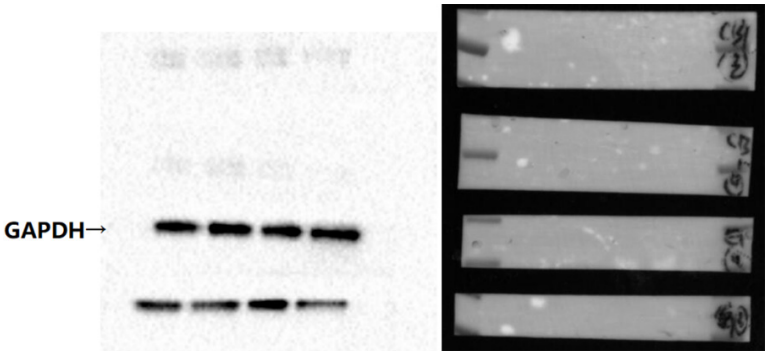

Supplementary Figure 4. The original full scan the entire original gel for GAPDH in **Figure 2D**.

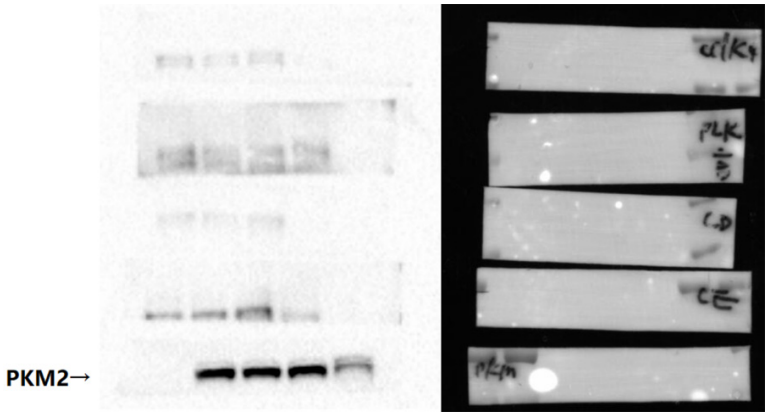

Supplementary Figure 5. The original full scan the entire original gel for PKM2 in **Figure 2D**.

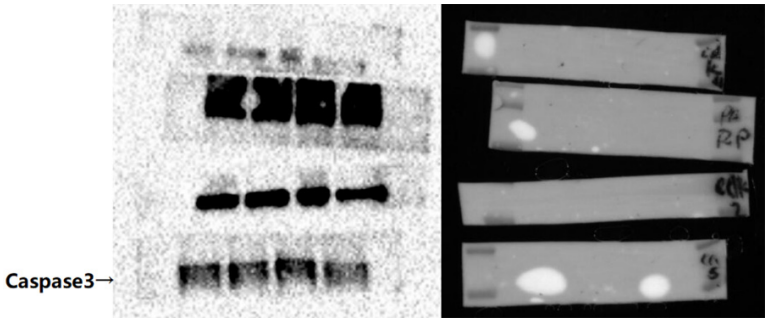

Supplementary Figure 6. The original full scan the entire original gel for caspase3 in **Figure 3C**.

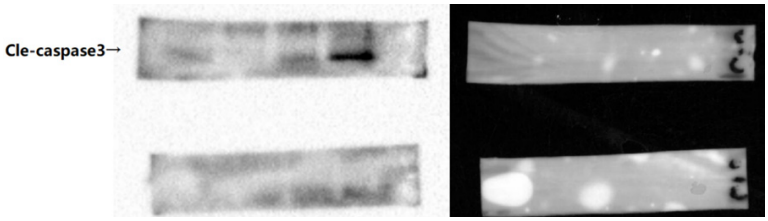

Supplementary Figure 7. The original full scan the entire original gel for Cle-caspase3 in **Figure 3C**.

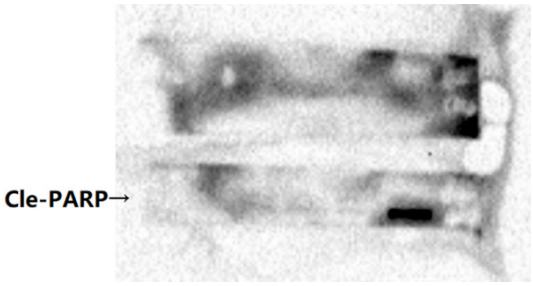

Supplementary Figure 8. The original full scan the entire original gel for Cle-PARP in **Figure 3C**.

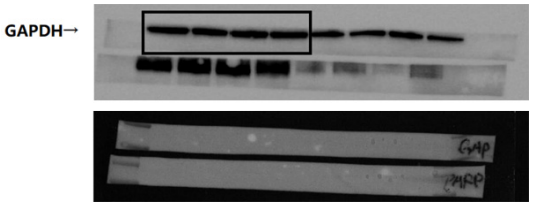

Supplementary Figure 9. The original full scan the entire original gel for GAPDH in **Figure 3C**.

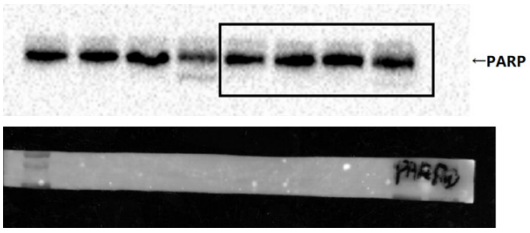

Supplementary Figure 10. The original full scan the entire original gel for PARP in **Figure 3C**.

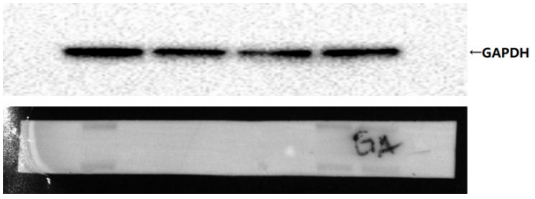

Supplementary Figure 11. The original full scan the entire original gel for GAPDH in **Figure 4A**.

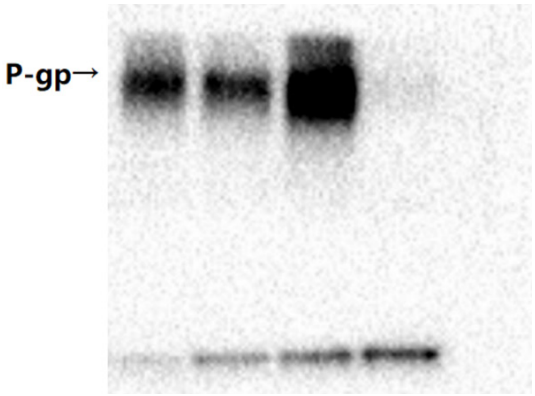

Supplementary Figure 12. The original full scan the entire original gel for P-gp in **Figure 4A**.

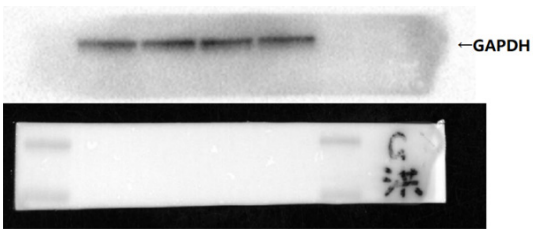

Supplementary Figure 13. The original full scan the entire original gel for GAPDH in **Figure 4B**.

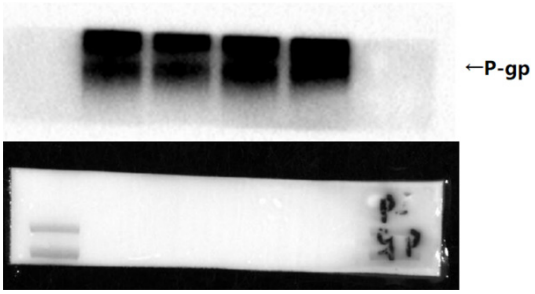

Supplementary Figure 14. The original full scan the entire original gel for P-gp in **Figure 4B**.